LABORATORY MODELLING OF CROSS-POLARIZED RADAR RETURN AT SEVERE WIND CONDITIONS

Yu.Troitskaya[1,2], V.Abramov[1], A.Ermoshkin[1], E.Zuikova[1], V.Kazakov[1,2], D.Sergeev[1,2], and A.Kandaurov[1]

Institute of Applied Physics, Nizhny Novgorod, Russian Federation
Nizhny Novgorod State University, Nizhny Novgorod, Russian Federation

ABSTRACT

Laboratory experiments directed to investigation of co-polarized and de-polarized X-band microwave radar return from the water surface at strong and hurricane wind were carried out in the high-speed wind-wave flume. Microwave measurements were accompanied by the measurements of air-flow and wave field parameters. Experiments showed that alternatively to the co-polarized return, the dependency of the de-polarized return on the wind speed do not saturate, although the growth rate decreases at wind speed exceeding 30 m/s. Comparison of the of the experimental data with the composite-surface Bragg scattering model for the measured parameters of the wind and waves showed, that the model is in agreement with measurements of microwave co-polarized return, but fails to describe the de-polarized radar return. The obtained dependency of de-polarized radar return was compared with the empirical geophysical model function based on collocated airborne and satellite data.

Index Terms— co-polarized and depolarized radar return; hurricane wind speed

1. INTRODUCTION

Satellite remote sensing is one of the main techniques of monitoring severe weather conditions over the ocean. Surface wind velocity is routinely measured by microwave scatterometers using co-polarized radar return due to sufficiently high intensity of the return signal. The existing algorithms of retrieving wind speed from scatterometry are based on dependence of microwave backscattering cross-section on wind speed (Geophysical Model Function, GMF) [1, 2]. The principal difficulty of these algorithms arises from saturation of GMF at winds exceeding 25 m/s [3]. Then the accuracy of wind speed retrieval ceases for severe winds like in hurricanes and typhoons.

Recently analysis of dual- and quad-polarization C-band radar return measured from satellite Radarsat-2 with co-located concomitant direct measurements of wind from oceanographic buoys NDBC [4-8], suggested that the cross-polarized radar return does not saturate at higher winds and it has much higher sensitivity to the wind speed than co-polarized back-scattering.

In the very recent paper [9] the GMF for cross-polarized radar cross-section (VH) was derived on the basic of RADARSAT-2 SAR images acquired during hurricanes collocated with airborne wind measurements by Stepped-Frequency Microwave Radiometer (SFMR) [10] made by NOAA's Hurricane Hunter flights. Since complete collocation of these data was not possible and time difference in flight legs and SAR images acquisition was up to 3 hours, these two sets of data were compared in [9] only statistically.

The main purpose of this paper is investigation of the functional dependence of cross-polarized radar cross-section on the wind speed by a laboratory experiment. Since cross-polarized radar return is formed at small-scale features at the air-sea interface (short-crested waves, foam, sprays, etc), which are well reproduced in laboratory conditions, then the approach based on laboratory experiment on radar scattering of microwaves at the water surface under hurricane wind looks appropriate.

2. EXPERIMENTAL FACILITY

The experiments were performed in the Wind-wave flume, which is the part of the Large Thermostratified Tank of the Institute of Applied Physics [11]. The working straight part of the flume is 10 m and operating cross section is 0.40×0.40 m^2, the axis velocity can be varied from 5 to 25 m s^{-1}, which corresponds to U_{10} from 7 m s^{-1} to 40 m s^{-1}.

2.1. Measurements of wind and waves

Parameters of the air flow in the turbulent boundary layer (friction velocity u_* and roughness height z_0) were retrieved by velocity profiling and subsequent data processing based on self-similarity of the turbulent boundary layer in the flume described in [11]. Then the equivalent 10-m wind speed was calculated by definition: $U_{10}=2.5u_*\ln(10m/z_0)$.

The wind wave field parameters in the flume were measured by three wire gauges positioned in the corners of an equal-side triangle with 2.5 cm side, the data sampling

rate was 100 Hz. For estimations of the cm-band wave spectra data from the extra wave-gauge with the 0.8 cm base were used. Three dimensional frequency-wave-number spectra $S(\omega,k,\theta)$ were retrieved from these data by the Fourier directional method (FDM) [11]. Integrating $S(\omega,k,\theta)$ over frequency yields wavenumber $S(k,\theta)$ directional spectra respectively. Integrating over θ gives frequency spectra and the wavenumber spectra correspondingly. Saturation wavenumber spectrum of the waves at the working section for different wind speeds U_{10} are shown in fig.1a. Estimations show that the high frequency part of the saturation wave-number spectrum at 1 cm^{-1}<k<4 cm^{-1} can be approximated as follows:

$$B(k,\theta)=2/\pi\alpha k^{\beta}\cos^2(\theta), \quad (1)$$

where the dependence of α and β on U_{10} are shown in fig 1b.

Also slope probability density function for "long waves" for comparing with the composite Bragg theory of microwave radar return according to [12, 13]. When calculating the slope probability density function (PDF) of "long waves" from experimental data, the dividing scale was set equal to three Bragg wavelengths. Note that the peculiarity of wind waves in this experiment was its high degree of nonlinearity and linear filtering of data was expected to lead to a strong distortion of the waveform. In this regard, for discrimination of the "long waves" the empirical mode decomposition (EMD) [14] was implemented. Taking into account that time series of the water surface elevations are characterized by a high degree of intermittency [15], the algorithm of Ensemble EMD (EEMD) was applied [16], which allows avoiding the phenomenon of "mixing modes. When constructing the slope PDF for "long waves" from the original time series of water surface elevations high-frequency intrinsic mode functions were subtracted in accordance with the criterion of the scale separation. Strong nonlinearity of the "long waves" resulted, in particular, in markedly difference of slope PDF from the Gaussian distribution.

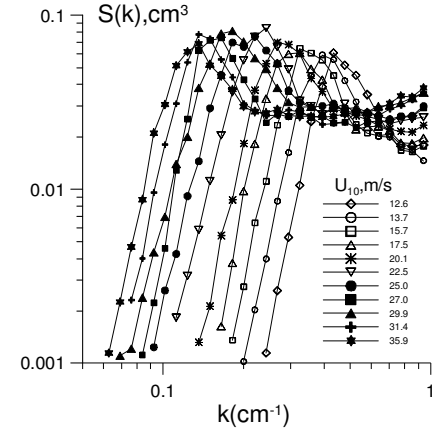

(a)

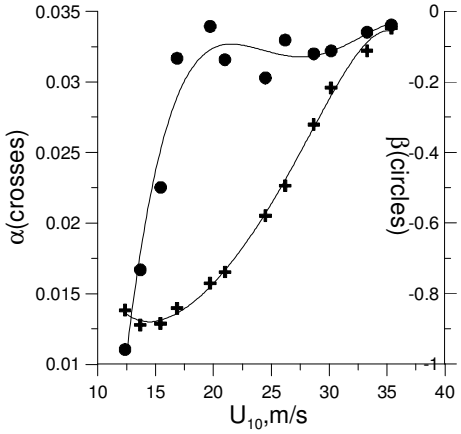

(b)

Fig.1 Saturation wavenumber spectrum of the waves at the working section for different wind speeds $U_{10.}$ (a), dependencies of α and β in equation (1) on U_{10} (b).

2.2. Microwave measurements

Microwave measurements were carried out by a coherent Doppler X-band (3.2 cm) scatterometer with the consequent receive of linear polarizations. Antenna was an optimized pyramidal horn with square cross-section 224×224 mm^2 and a length 680mm, which is equipped with the orthomode transducer with isolation of polarizations of more than 40 dB; the beam-width was 9°. The absolute value of the radar cross-section (RSC) of rough water surface was determined by comparing the scattered signal with the signal reflected from the reference reflector (calibrator) with the known value of the RCS - a metal ball-pendulum 6 cm in diameter.

Principal scheme of the experimental setup in working section at a distance of 6 m from the inlet is shown in fig.2.

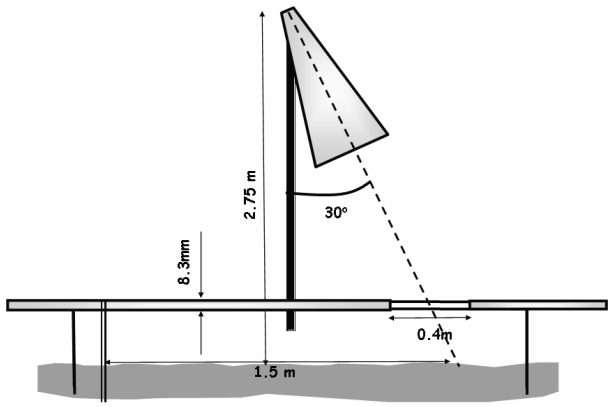

Рис.2. Principal scheme of the experimental setup in the working section for microwave measurements.

The observation window was 40x40 cm^2, incidence angle 30 deg, distance from the target was 3.16 m at the height 2.75

m from the water, thickness of the plexiglas of the flume was 8.3mm. To reduce the influence of reflections taken from the side lobes, the most "critical" reflectors of the tank were covered with pieces of radio-absorbing material.

3. RESULTS OF EXPERIMENTS AND GEOPHYSICAL MODEL FUNCTION

The dependencies of normalized radar cross-section (NRSC) in linear units for 4 polarizations is shown in fig.3. One can see that the cross-polarized radar return is two orders lower

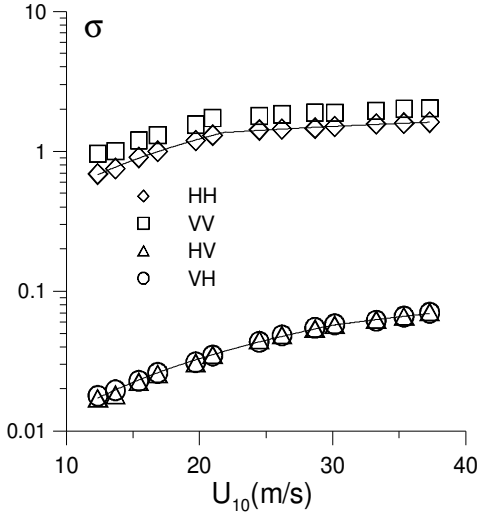

Fig.3. Co-polarized and de-polarized NRSC via wind speed, incidence angle is 30°.

than the co-polarized one, has higher sensitivity to the wind speed. Indeed, the cross-polarized radar cross-section σ_{VH} at U_{10}<30 m/s grows proportionally to $(U_{10})^{1.5}$, while σ_{VV} and σ_{HH} are proportional to $(U_{10})^{0.9}$. At wind speeds exceeding 30m/s, the cross-polarized radar return growth slows down and becomes proportionally to $(U_{10})^{0.7}$, while σ_{VV} and σ_{HH} are saturated. We also notice that co-polarized radar return at vertical polarization σ_{VV} exceeds the horizontal one σ_{HH} with the polarization difference about 1-2 dB in agreement with [].

In fig.4 we compared measured σ_{0PQ} (here P and Q denotes different polarizations and equals to H or V) with the predictions of composite Bragg theory (Valensuela, 1978, Plant, 1990), where the spectral density of surface waves and probability density function for "long waves" were taken from measurements of the wave field. In this configuration of experimental setup the Bragg wave length was λ_b=3.2 cm and cut-off wave length was $5\lambda_b$.

One can see that for co-polarized radar returns the difference with the model is about 1-2 dB and it can be explained by our poor knowledge about the short wave part of the spectrum. For cross-polarized return the difference exceeds 10 dB, and it means that some non-Bragg mechanisms (short-crested waves, foam, sprays, etc) are responsible for the depolarization of the returned signal. Then it seems reasonable to compare the dependence of cross-polarized X-band radar cross section on 10-m wind speed obtained in laboratory conditions with the similar dependence obtained in [9] from the field data for C-band radar cross-section.

In Fig. 5 we superimpose the laboratory X-band data with the distribution of all retrieved SFMR wind speeds

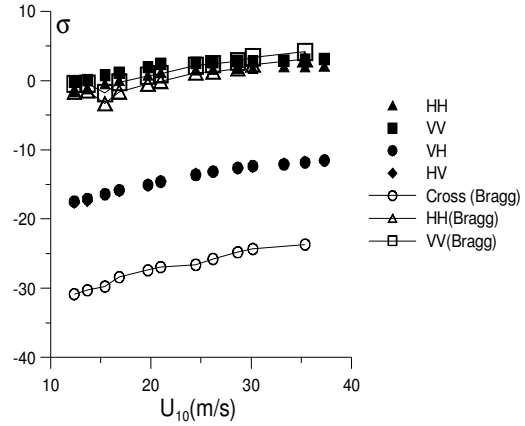

Fig.4. Comparison of measured co-polarized and cross-polarized radar cross-sections and predictions of composition Bragg model.

versus collocated VH measurement points from 9 hurricanes (top panel of Fig.3 from [9]. One can see that the laboratory data follow the median of the field data with the constant bias 11 dB. Fitting the experimental data by polynomial curves gives the GMF obtained for incidence angle 30° and azimuth angle 0°. Best fit line for X -band date gives

$$\sigma_{VH}^{X} = \begin{cases} -21 + 0.33U_{10}, for 20 < U_{10} < 30, \\ -19 + 0.39U_{10} - 0.0046U_{10}^2, for U_{10} > 30. \end{cases}$$

Taking into account the constant bias 11 dB gives for C-band

$$\sigma_{VH}^{C} = \begin{cases} -32 + 0.33U_{10}, for 20 < U_{10} < 30, \\ -30 + 0.39U_{10} - 0.0046U_{10}^2, for U_{10} > 30. \end{cases}$$

4. CONCLUSIONS

Laboratory experiments directed to investigation of co-polarized and cross-polarized X-band microwave radar return from the water surface at strong and hurricane wind were carried out. Parameters of air-flow velocity (wind friction velocity and roughness height) and surface wind waves (spectra and probability density function of slopes) in the laboratory facility were retrieved from simultaneous measurements. It was shown that alternatively to the co-polarized return, the dependency of the cross-polarized return on the wind speed is unambiguous, although the growth rate of radar cross-section on wind speed decreases at wind speed exceeding 30 m/s.

We compared the dependency of the cross-polarized X-band radar cross-section on wind speed obtained in

laboratory with the similar dependency retrieved from Radarsat-2 SAR images and collocated airborne SFMR wind measurements [8]. We found out that the laboratory data follow the median of the field data with the constant bias 11 dB. Basing on laboratory data an empirical geophysical

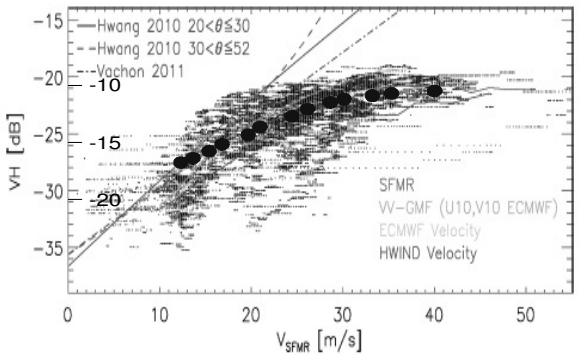

Fig.5 Distribution of all retrieved SFMR wind speeds versus collocated VH measurement points from 9 hurricanes (top panel of Fig.3 from [8]) and superimposed laboratory data (blue points).

model function was suggested for retrieving wind speed up to 40 m/s from cross-polarized microwave return, which is in good agreement with the direct measurements.

5. ACKNOWLEGEMENTS

Microwave experiments and data processing were carried out under financial support of the RSF (project 14-17-00667), wave measurements were supported by RFBR (projects 13-05-00865, 12-05-12093), equipment was provided by grant from the Government of the Russian Federation (project code 11.G34.31.0048).

REFERENCES

[1] H. Hersbach, “Comparison of C-band scatterometer CMOD5.N equivalent neural winds with ECMWF”. J. Atmos. Oceanic Technol, pp. 721–736, v. 27, 2010.

[2] H. Hersbach, A. Stoffelen, and S. de Haan “An improved C-band scatterometer ocean geophysical model function: CMOD5”. J. Geophys. Res., 112, C03006, 2007.

[3] W.J.Donnelly, J. R. Carswell, R. E. McIntosh, P. S. Chang, J. Wilkerson, F. Marks, and P. G. Black “Revised ocean backscatter models at C and Ku band under high-wind conditions”, J. Geophys. Res., 104(C5), 11485–11497, doi:10.1029/1998JC900030, 1999.

[4] Hwang, P. A., B. Zhang, and W. Perrie, (2010) Depolarized radar return for breaking wave measurement and hurricane wind retrieval. Geophys. Res. Lett., 37, L01604, doi:10.1029/2009GL041780.

[5] P. A. Hwang, B. Zhang, J. V. Toporkov, and W. Perrie, “Comparison of composite Bragg theory and quad-polarization radar backscatter from RADARSAT-2: With applications to wave breaking and high wind retrieval”. J. Geophys. Res., doi:10.1029/2009JC005995, 2010

[6] B. Zhang, , W. Perrie, and Y. He, “Wind speed retrieval from RADARSAT-2 quad-polarization images using a new polarization ratio model.” J. Geophys. Res., 116, C08008, doi:10.1029/2010JC006522, 2011

[7] P. W.Vachon, and J. Wolfe “C-band cross-polarization wind speed retrieval”. IEEE Geosci. Remote Sens. Lett., 8, 456–459, 2011.

[8] B. Zhang, W. Perrie “Cross-Polarized Synthetic Aperture Radar: A New Potential Measurement Technique for Hurricanes”. Bull. Amer. Meteor. Soc., 93, 531–541, 2012.

[9] G.-J. van Zadelhoff, , A. Stoffelen, P.W.Vachon, J.Wolfe, J.Horstmann, and M. Belmonte Rivas “Scatterometer hurricane wind speed retrievals using cross polarization”, Atmos. Meas. Tech. Discuss., 6, 7945-7984, doi:10.5194/amtd-6-7945-2013, 2013.

[10] Uhlhorn, E. W., Black, P. G., Franklin, J. L., Goodberlet, M., Carswell, J., and Goldstein, A. S.:”Hurricane surface wind measurements from an operational stepped frequency microwave radiometer”, Mon. Weather Rev., 135, 3070–3085, doi:10.1175/MWR3454.1, 2007.

[11] Troitskaya, Y. I., D. A. Sergeev, A. A. Kandaurov, G. A. Baidakov, M. A. Vdovin, and V. I. Kazakov “Laboratory and theoretical modeling of air-sea momentum transfer under severe wind conditions” J. Geophys. Res., 117, C00J21, 2012.

[12] G. R. Valenzuela (1978) "Theories for the interaction of electromagnetic and oceanic waves— A review," Boundary-Layer Meteorology, 13, 61-85.

[13] Plant, W. J., Bragg scatteringo f electromagneticw avesf rom the air/sea interface, in Surface Waves and Fluxes, edited by G. L. Geernaert and W. J. Plant, pp. 41-108, Kluwer Academic, Norwell, Mass., 1990.

[14] N. E. Huang, Z. Shen, S. R. Long, M. C. Wu, E. H. Shih, Q. Zheng, C. C. Tung and H. H. Liu, The empirical mode decomposition method and the Hilbert spectrum for non-stationary time series analysis, Proc. Roy. Soc. London 454A (1998) 903–995.

[15] N. E. Huang, Z. Shen and R. S. Long, A new view of nonlinear water waves — the Hilbert spectrum, Ann. Rev. Fluid Mech. 31 (1999) 417–457.

[16] Wuand, Z., Huang, N. E.: Ensemble Empirical Mode Decomposition and Noise-assisted Data Analysis Method, World Scientific Publishing Copany, Advances in Adaptive Data Analysis, Vol. 1, No. 1 (2009), p. 1–41.